

## Inertial Oscillations and the DuFort-Frankel Difference Scheme

FRANK B. LIPPS

*Geophysical Fluid Dynamics Laboratory/NOAA, Princeton University, Princeton, New Jersey 08540*

Received November 4, 1974; revised August 25, 1976

The present study examines the problem of horizontally uniform inertial oscillations in a homogeneous, horizontally unbounded rotating fluid. The analytical solution indicates that these oscillations are damped in time due to viscosity. Numerical calculations using the DuFort-Frankel finite difference scheme indicate that amplifying numerical solutions can exist when high frequency inertial oscillations are present. These positive growth rates are associated with the finite difference second time derivative which is a part of this scheme. The amplifying solutions can be eliminated by using a sufficiently small time step  $\Delta t$ . The existence of such solutions was encountered in a study of three-dimensional Bénard convection in a rotating fluid. The numerical results and primary conclusions of that study are summarized.

### 1. INTRODUCTION

In numerical calculations there are several methods of taking the finite difference forms of the viscous and diffusive terms in the hydrodynamical equations of motion. One of these methods is the DuFort-Frankel difference scheme, which is usually analyzed with respect to the heat equation (see [4, 5]). For this case the DuFort-Frankel scheme is stable for any value of the time step  $\Delta t$ , although the accuracy decreases for large  $\Delta t$ . In the present study a problem is considered for which high frequency inertial oscillations can exist. The analytical solution indicates that these oscillations are damped in time. It is shown, however, that using the DuFort-Frankel scheme amplifying numerical solutions can develop. Although no proof is given, the present investigator considers it likely that similar amplifying modes can exist for other types of high frequency oscillations as well.

In Section 2, a simplified dynamical problem involving the motion in a homogeneous rotating fluid is formulated. The fluid is confined between two planes in the vertical and is unbounded in the horizontal. High frequency inertial oscillations can exist when the rotation rate is sufficiently large. The numerical solution of this problem applies the DuFort-Frankel difference scheme to represent the viscous terms in the equations of motion. Due to the artificial second time derivative associated with this scheme (see [4] or [5]), amplifying solutions will develop if the time step  $\Delta t$  is not sufficiently small.

In Section 3, a previous study [8] is discussed in which three-dimensional numerical calculations were performed to simulate Bénard convection in a rotating fluid. The

mathematical formulation of the rotating Bénard problem is given, and the primary numerical results and conclusions are summarized. For the case of highest rotation, an amplifying mode developed which was of the same form as analyzed in Section 2. When the time step  $\Delta t$  was reduced, this mode was not observed and the numerical results were realistic.

## 2. DUFORT-FRANKEL INSTABILITY FOR A ROTATING HOMOGENEOUS FLUID

The general problem is first specified and the analytical solution given. The numerical problem is then discussed. A homogeneous fluid is unbounded in the horizontal and confined between two planes, separated by the distance  $d$ , in the vertical. The fluid has a constant coefficient of kinematic viscosity  $\nu$ . The planes are assumed to rotate about the vertical axis with the rotation rate  $\Omega$ . The hydrodynamical equations of motion are specified in a coordinate system rotating with the two planes. The origin of the coordinates is located on the lower plane.

### 2.1. The Analytical Solution

Inertial solutions are considered for which the horizontal velocities are functions of the vertical coordinate  $z$  and the time  $t$  only. The horizontal pressure gradients are assumed to be zero everywhere. The vertical velocity  $w$  must vanish identically due to the constraint of continuity and the two rigid boundaries in the vertical. The nonlinear terms in the momentum equations also vanish identically. Cartesian coordinates  $(x, y, z)$  are defined with the corresponding velocities  $(u, v, w)$ . The horizontal momentum equations for  $u$  and  $v$  are given by

$$\partial u / \partial t = 2\Omega v + \nu(\partial^2 u / \partial z^2), \quad (1a)$$

$$\partial v / \partial t = -2\Omega u + \nu(\partial^2 v / \partial z^2). \quad (1b)$$

The no-slip conditions  $u = v = 0$  are required to be satisfied at the boundaries located at  $z = 0$  and  $z = d$ .

The above problem has a solution of the form

$$u = u_0 e^{\sigma t} \sin mz, \quad (2a)$$

$$v = v_0 e^{\sigma t} \sin mz, \quad (2b)$$

where  $m = \pi/d$  and  $u_0, v_0$  are constants determined by the initial conditions at  $t = 0$ . The time dependence can be obtained by substituting (2a), (2b) into (1a), (1b) and setting the determinant of the coefficients equal to zero. The resulting quadratic equation in  $\sigma$  gives the solutions

$$\sigma = \pm i2\Omega - \nu m^2. \quad (3)$$

Thus the imaginary part of these solutions indicates the presence of inertial oscillations with the frequency  $2\Omega$ . However, for any homogeneous fluid with a nonzero viscosity  $\nu$ , these oscillations will be damped in time.

## 2.2. Formulation of the Numerical Problem

The finite difference form of Eqs. (1a) and (1b) must be specified for the numerical problem. The terms  $\partial u/\partial t$ ,  $2\Omega v$ , and  $\nu(\partial^2 u/\partial z^2)$  in (1a) are represented by

$$\frac{\partial u}{\partial t} \approx \frac{1}{2\Delta t} (u_k^{n+1} - u_k^{n-1}), \quad (4a)$$

$$2\Omega v \approx 2\Omega v_k^n, \quad (4b)$$

$$\nu \frac{\partial^2 u}{\partial z^2} \approx \frac{\nu}{(\Delta z)^2} \{u_{k+1}^n - u_k^{n+1} - u_k^{n-1} + u_{k-1}^n\}, \quad (4c)$$

where  $\Delta t$  is the time step,  $\Delta z$  is the vertical grid interval, and  $n, k$  are integers related to  $t$  and  $z$  such that  $t = n \Delta t$  and  $z = k \Delta z$ . A similar representation is used for the terms in (1b).

Thus, the finite difference forms of  $\partial u/\partial t$  and  $\partial^2 u/\partial z^2$  given in (4a) and (4c) are specified according to the DuFort-Frankel scheme. Note that the finite difference form of  $\partial^2 u/\partial z^2$  can be rewritten as

$$\frac{\partial^2 u}{\partial z^2} \approx \frac{1}{(\Delta z)^2} \{u_{k+1}^n + u_{k-1}^n - 2u_k^n\} - \beta^2 \frac{1}{(\Delta t)^2} \{u_k^{n+1} + u_k^{n-1} - 2u_k^n\} \quad (5)$$

where  $\beta = \Delta t/\Delta z$ . As discussed in [4, 5], the right-hand side of (5) is consistent with  $\partial^2 u/\partial z^2$  if and only if  $\beta \rightarrow 0$  as  $\Delta t \rightarrow 0$ . If  $\beta$  approaches a constant as  $\Delta t \rightarrow 0$ , then the right-hand side of (5) is consistent with

$$(\partial^2 u/\partial z^2) - \beta^2(\partial^2 u/\partial t^2).$$

Thus, for finite  $\Delta t$  and  $\Delta z$ , the second term on the right side of Eq. (5) represents an artificial finite difference second time derivative. It will be shown below that the existence of a finite  $\beta$  can lead to the existence of amplifying numerical solutions.

The following analysis makes two basic assumptions. These are that the time step  $\Delta t \sim \frac{1}{2}(\Delta z)^2/\nu$  and that the inertial oscillations are reasonably well resolved. Specifically it is assumed that

$$\gamma = \frac{2\nu \Delta t}{(\Delta z)^2} = O(1), \quad 2\Omega \Delta t = \epsilon^{1/2}. \quad (6)$$

Note that  $\gamma$  can also be written as  $2\nu\beta^2/\Delta t$ . In order to have an idea of expected magnitudes of  $\gamma$  and  $\epsilon$ , the Bénard problem discussed in Section 3 is considered. In particular, the case of highest rotation with the Taylor number  $T = 10,000$  as shown in Table I is examined. It is found for this case that  $\gamma = 0.87$  and  $\epsilon = 0.029$ .

The finite difference equations corresponding to (1a), (1b) have solutions of the form

$$u = u_o \exp(\sigma_N t) \sin mz, \quad (7a)$$

$$v = v_o \exp(\sigma_N t) \sin mz, \quad (7b)$$

where again  $t = n \Delta t$  and  $z = k \Delta z$ . The complex numerical frequency is represented by  $\sigma_N$ . These solutions satisfy the no-slip boundary conditions  $u = v = 0$  at  $z = 0$  and  $z = d$ .

TABLE I<sup>a</sup>  
Details of the Four Numerical Integrations [8]

Run	$\Delta t$	$t_c$	$N$	$N_e$	$\lambda$	$\lambda_e$
$T = 0$	$0.45 \times 10^{-3}$	0.675	2.56	2.58	2.76	2.4
$T = 400$	$0.45 \times 10^{-3}$	0.540	2.72	2.63	2.33	2.4
$T = 2500$	$0.45 \times 10^{-3}$	0.742	2.85	2.75	1.44	1.8-1.9
$T = 10,000$	$0.25 \times 10^{-3}$	0.345	2.67	2.57	1.36	1.4-1.5

<sup>a</sup> The time step  $\Delta t$  and the total time of the run  $t_c$  are scaled by  $d^2/\kappa$ . The experimental values  $N_e$  and  $\lambda_e$  were obtained from Rossby [6].

### 2.3. The Existence of Amplifying Solutions

In Section 2.1 it was shown that the analytical solutions for the inertial oscillations are damped in time. For this reason, the primary concern of the present analysis is to determine whether neutral or amplifying numerical solutions exist for the finite difference equations. It will be shown that such solutions do exist under certain conditions.

If we substitute (7a), (7b) into the finite difference counterparts of (1a), (1b) and set the determinant of the coefficients equal to zero, we find

$$S_1 + \nu(M^2 + \beta^2 S^2) = \pm 2\Omega i \quad (8)$$

where  $S_1$ ,  $S$ , and  $M^2$  are given by

$$S_1 = \frac{1}{\Delta t} \sinh(\sigma_N \Delta t), \quad (9a)$$

$$S^2 = \frac{2}{(\Delta t)^2} (\cosh(\sigma_N \Delta t) - 1), \quad (9b)$$

$$M^2 = \frac{2}{(\Delta z)^2} (1 - \cos(m \Delta z)). \quad (9c)$$

The complex  $\sigma_N$  is defined by

$$\sigma_N = \sigma_{Nr} + i\sigma_{Ni}. \quad (10)$$

Using this definition, (8) can be separated into its real and imaginary parts

$$\cos(\sigma_{Ni} \Delta t) \{ \sinh(\sigma_{Nr} \Delta t) + \gamma \cosh(\sigma_{Nr} \Delta t) \} = \gamma - \Delta t \nu M^2, \quad (11a)$$

$$\sin(\sigma_{Ni} \Delta t) \{ \cosh(\sigma_{Nr} \Delta t) + \gamma \sinh(\sigma_{Nr} \Delta t) \} = \pm 2\Omega \Delta t. \quad (11b)$$

The imaginary component  $\sigma_{Ni}$  of  $\sigma_N$  can be eliminated from (11a), (11b) through use of the equation

$$\cos^2(\sigma_{Ni} \Delta t) + \sin^2(\sigma_{Ni} \Delta t) = 1. \quad (12)$$

After some algebra, the following equation is obtained

$$\begin{aligned} & -\nu M^2 \left( 1 - \frac{(\Delta z)^2 M^2}{4} \right) + 4\Omega^2 \beta^2 \nu h(\sigma_{Nr} \Delta t) \\ & = \frac{\gamma}{2\Delta t} \left\{ \left( \frac{1}{\gamma} \sinh(\sigma_{Nr} \Delta t) + \cosh(\sigma_{Nr} \Delta t) \right)^2 - 1 \right\} \end{aligned} \quad (13)$$

where

$$h(\sigma_{Nr} \Delta t) = \frac{(1 + (1/\gamma) \tanh(\sigma_{Nr} \Delta t))^2}{(1 + \gamma \tanh(\sigma_{Nr} \Delta t))^2}. \quad (14)$$

The function  $h(\sigma_{Nr} \Delta t)$  is either monotonic increasing or decreasing, with  $h(0) = 1$  and  $h(\infty) = (1 + 1/\gamma)^2 / (1 + \gamma)^2$ .

The left side of (13) is denoted by the function  $f(\sigma_{Nr})$  and the right side by  $g(\sigma_{Nr})$ . A solution exists whenever  $f = g$ . If  $\sigma_{Nr} = 0$ , then  $g = 0$  and  $h = 1$  so that a solution exists when  $f = 0$ , or

$$-M^2 \left( 1 - \frac{(\Delta z)^2}{4} M^2 \right) + 4\Omega^2 \beta^2 = 0. \quad (15)$$

This is the condition for neutral disturbances to exist.

The functions  $f$  and  $g$  are drawn schematically for positive  $\sigma_{Nr}$  in Fig. 1. The function  $g(\sigma_{Nr})$  monotonically increases from zero to infinity as  $\sigma_{Nr}$  increases from zero to infinity. The function  $f(\sigma_{Nr})$  remains finite for all positive  $\sigma_{Nr}$ . In Fig. 1  $f(0) > 0$  is assumed. This figure clearly shows that a positive growth rate  $\sigma_{Nr} = \sigma_1$  exists when  $f(0) > 0$ .

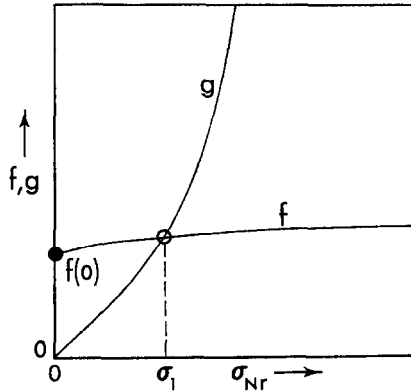


FIG. 1. The plot of  $f$  and  $g$  (from Eq. (13)) as functions of positive  $\sigma_{Nr}$ . See text for discussion.

The remaining question is whether amplifying solutions can exist if  $f(0) < 0$ . To answer this question, the derivatives of  $g$  and  $f$  with respect to  $\sigma_{Nr}$  are calculated for  $\sigma_{Nr} \geq 0$

$$dg/d\sigma_{Nr} = \cosh^2(\sigma_{Nr} \Delta t)(1 + (1/\gamma) \tanh(\sigma_{Nr} \Delta t))(1 + \gamma \tanh(\sigma_{Nr} \Delta t)), \quad (16)$$

$$df/d\sigma_{Nr} = \epsilon(1 - \gamma^2) \frac{(1 + (1/\gamma) \tanh(\sigma_{Nr} \Delta t))(1 - \tanh^2(\sigma_{Nr} \Delta t))}{(1 + \gamma \tanh(\sigma_{Nr} \Delta t))^3}. \quad (17)$$

A comparison of (16) and (17) shows that  $df/d\sigma_{Nr} < dg/d\sigma_{Nr}$  for  $\sigma_{Nr} > 0$  if  $\epsilon(1 - \gamma^2) < 1$ . But  $\epsilon$  is a small quantity and  $\gamma = O(1)$  so that the condition  $\epsilon(1 - \gamma^2) < 1$  will be met. Thus if  $f(0) < 0$ , there is no possibility that the  $f(\sigma_{Nr})$  curve can cross the  $g(\sigma_{Nr})$  curve for  $\sigma_{Nr} > 0$ . Hence amplified solutions exist if and only if  $f(0) > 0$ . These solutions can be eliminated by requiring  $\Delta t$  to be sufficiently small so that  $f(0) \leq 0$ . The condition

$$\Delta t < M \left(1 - \frac{(\Delta z)^2}{4} M^2\right)^{1/2} (\Delta z/2\Omega) \quad (18)$$

will insure that damped solutions will only exist.

It is of interest to simplify expression (18). From definition (9c) of  $M^2$  and the definition  $m = \pi/d$ , it can be shown that to order  $(\Delta z/d)^2$

$$M \left(1 - \frac{(\Delta z)^2}{4} M^2\right)^{1/2} \simeq m \left(1 - \frac{\pi^2}{6} \left(\frac{\Delta z}{d}\right)^2\right). \quad (19)$$

Thus for good resolution in the vertical (ten grid points or more)

$$M \left(1 - \frac{(\Delta z)^2}{4} M^2\right)^{1/2} \simeq m \quad (20)$$

and (18) is simplified to

$$\Delta t < (m/2\Omega) \Delta z. \quad (21)$$

Now define the wavelength  $\lambda = 2\pi/m$  and the inertial period  $\tau = \pi/\Omega$ . Then (21) becomes

$$\Delta t/\tau < \Delta z/\lambda. \quad (22)$$

For stable solutions to exist, the above equation indicates that the number of time steps  $\Delta t$  required to resolve the period  $\tau$  is equal or greater than the number of grid intervals used to resolve the wavelength  $\lambda$ . Thus, the existence of amplifying solutions does not necessarily indicate that the numerical resolution of  $\tau$  is poor. It rather indicates that the resolution of  $\tau$  is not as good as that of  $\lambda$ .

In conclusion, we note that amplifying modes can occur for high frequency inertial waves even if  $\beta$  is relatively small. Although no proof is given, this investigator is of the opinion that amplifying modes are also possible when other types of high frequency oscillations are present.

### 3. NUMERICAL SIMULATION OF BÉNARD CONVECTION IN A ROTATING FLUID

The present investigator has encountered numerical difficulties with the DuFort-Frankel scheme for two separate studies. The first was a joint effort by Somerville and Lipps [8] to numerically simulate Bénard convection in a rotating fluid. This study and the numerical difficulties associated with it will be discussed in Sections 3.1 and 3.2. In the second study [2], calculations were carried out to simulate Bénard convection in air. The accuracy of the DuFort-Frankel scheme for those calculations is discussed in detail in Appendix B of that study.

#### 3.1. Formulation of the Problem and the Numerical Model

The present Bénard convection problem involves a horizontally unbounded fluid confined between two rigid horizontal plates. These are maintained at different constant temperatures, the lower one being the warmer. The plates are also subject to a uniform rotation rate about a vertical axis. The specification of the problem is conventional [1] and involves eight constants. These are the depth of the fluid layer  $d$ , the acceleration of gravity  $g$ , the temperature difference  $\Delta\theta$  across the layer, the angular rate of rotation  $\Omega$ , the mean density  $\rho_0$ , and the coefficients  $\alpha$ ,  $\kappa$ , and  $\nu$  of thermal expansion, thermometric conductivity, and kinematic viscosity.

Three independent dimensionless parameters which are important in the present problem are the Rayleigh number  $R$ , the Taylor number  $T$ , and the Prandtl number  $P$ :

$$R = g\alpha \Delta\theta d^3/\nu\kappa, \quad T = 4\Omega^2 d^4/\nu^2, \quad P = \nu/\kappa.$$

The equations and boundary conditions are given in dimensionless form with the Cartesian coordinates  $(x, y, z)$  scaled by  $d$ , the time  $t$  scaled by  $d^2/\kappa$ , the vector velocity  $\mathbb{V}$  scaled by  $\kappa/d$ , the temperature  $\theta$  scaled by  $\Delta\theta$ , and the pressure  $p$  scaled by  $\rho_0\kappa/d$ . The equations for conservation of mass, momentum, and thermodynamic energy then become

$$\nabla \cdot \mathbb{V} = 0, \quad (23)$$

$$(\partial\mathbb{V}/\partial t) + \mathbb{V} \cdot \nabla\mathbb{V} + PT^{1/2}\mathbb{K}X\mathbb{V} + \nabla p - P\nabla^2\mathbb{V} - PR\theta\mathbb{K} = 0, \quad (24)$$

$$(\partial\theta/\partial t) + \mathbb{V} \cdot \nabla\theta - \nabla^2\theta = 0. \quad (25)$$

Here  $\mathbb{K}$  is a unit vector, parallel to the vertical coordinate  $z$  and to the rotation axis and opposite in direction to gravity. The above equations are expressed in a coordinate system rotating with the boundaries. Taking the origin on the lower boundary, the conducting, no-slip boundary conditions are given by

$$\theta = \frac{1}{2}, \mathbb{V} = 0 \text{ at } z = 0; \quad \theta = -\frac{1}{2}, \mathbb{V} = 0 \text{ at } z = 1.$$

The numerical calculations are carried out in a finite volume specified by  $0 \leq x \leq L_x$ ,  $0 \leq y \leq L_y$ , and  $0 \leq z \leq 1$ . At the lateral side boundaries cyclic continuity is required at  $x = 0$  and  $x = L_x$  and at  $y = 0$  and  $y = L_y$ . The values  $L_x = 6.0$ ,  $L_y = 4.9$  and the grid intervals  $\Delta x = \Delta y = 0.1364$ ,  $\Delta z = 0.0625$  were used in [8]. The values used for the time step  $\Delta t$  will be discussed below.

The numerical procedure for the time integration of Eqs. (24) and (25) follows that described by Williams [9] and is discussed in detail in [2]. Of the most significance here is that the viscous and diffusive terms are evaluated using the DuFort–Frankel finite difference scheme. Since the Laplacian operators in (24) and (25) are three-dimensional, the form of  $\beta$  will be modified from that given in Section 2.2. The present form of  $\beta$  is denoted by  $\beta_1$  and is defined as

$$\beta_1 = \frac{\Delta t}{\Delta z} \left[ 1 + \left( \frac{\Delta z}{\Delta x} \right)^2 + \left( \frac{\Delta z}{\Delta y} \right)^2 \right]^{1/2}. \quad (26)$$

Using  $\beta_1$  the stability condition is somewhat more stringent than indicated by Eqs. (18) and (22). For example, Eq. (18) becomes

$$\Delta t < M_1 \left( 1 - \frac{(\Delta z)^2}{4} M_1^2 \right)^{1/2} \left( 1 + \left( \frac{\Delta z}{\Delta x} \right)^2 + \left( \frac{\Delta z}{\Delta y} \right)^2 \right)^{-1/2} T^{-1/2} P^{-1} \Delta z \quad (27)$$

where  $M_1 = Md$  for the present scaling.

### 3.2. Numerical Results and Primary Conclusions

The motivation for the calculations in [8] was to examine the nonmonotonic dependence of the heat transport on  $T$  as found experimentally by Rossby [6]. His result was not expected, since linear stability theory (1) suggests that rotation should decrease the intensity of the convection. Thus, the heat transport was expected to monotonically decrease with increasing rotation.

The four numerical runs carried out in [8] are summarized in Table I. These calculations were performed for  $R = 15,000$  and  $P = 6.8$  (water). In this table  $\Delta t$  is the time step and  $t_c$  is the total time of each run. The heat transport is expressed in terms of the Nusselt number  $N$ . This quantity can be defined in terms of the volume average

$$N = \frac{1}{L_x L_y} \int_0^1 \int_0^1 \int_0^{L_z} \left( w\theta - \frac{\partial \theta}{\partial z} \right) dx dy dz. \quad (28)$$

When no motion exists, the boundary conditions at  $z = 0$  and  $z = 1$  require  $N = 1$ . For finite amplitude Bénard convection  $N > 1$ .

The remaining parameter shown in Table I is the horizontal wavelength  $\lambda$  of the flow patterns. The experimental wavelengths  $\lambda_e$  were obtained as mean values from photographs taken by Rossby [6]. The numerical values of  $\lambda$  were obtained as mean values from the horizontal variation of  $w$  at the  $z = 0.5$  level.

Numerical and experimental values of  $N$  are shown in columns four and five of Table I. These data indicate that the numerical calculations reproduce the observed nonmonotonic dependence of  $N$  with  $T$ . The reason for this behavior of  $N$  appears to be related to the decrease in  $\lambda$  as  $T$  is increased. This variation of  $\lambda$  with  $T$  is seen in the final two columns of Table I. Two-dimensional calculations by Lipps and Somerville [3] show that for  $T = 0$  and  $R$  and  $P$  held fixed, a decrease in  $\lambda$  is associated with an increase in  $N$ . Thus, at small  $T$ , it appears that the increase in  $N$  is associated



with the decrease in  $\lambda$ . For larger values of  $T$ , the stabilizing effect of rotation becomes dominant so that  $N$  decreases with increasing  $T$ . This explanation of the observed variation of  $N$  with  $T$  was first suggested by Somerville [7]. A more detailed discussion of this conclusion and of the numerical results is given in [8].

As seen in Table I, the time step  $\Delta t = 0.45 \times 10^{-3}$  was used for all but the largest value of  $T$ . When calculations at  $T = 10,000$  were attempted using this value of  $\Delta t$ , an amplifying mode similar to those discussed earlier developed. Calculations were then performed at  $T = 10,000$  using  $\Delta t = 0.25 \times 10^{-3}$ . These calculations were well behaved with no observation of amplifying solutions. It should be noted that condition (27) requires the time step  $\Delta t < 0.2407 \times 10^{-3}$ . Thus, the value of  $\Delta t$  used was slightly larger than given by (27).

The calculations at  $T = 10,000$  remained stable either because the numerical scheme had stabilizing factors not included in the present analysis or because the amplifying solutions did not have time to develop. The latter explanation is likely because  $\Delta t$  is very near the critical value given by (27). Calculating  $f(0)$  and using  $dg/d\sigma_{Nr}|_0 = 1$  obtained from (16),  $\sigma_{Nr}$  can be approximately calculated and the amplification factor  $\exp(\sigma_{Nr}t_c)$  can be evaluated for unstable numerical disturbances growing during the total time  $t_c$  of the run. With  $t_c = 0.345$ , the amplification factor is calculated to be 6.0. This small value can easily explain why such disturbances had no importance in the calculations.

#### ACKNOWLEDGMENTS

A major credit for this paper has to go to an informal discussion between William R. Holland and the author at the Geophysical Fluid Dynamics Laboratory. The ideas brought out in that discussion ultimately led to the present manuscript. Thanks also go to Gareth Williams and Kirk Bryan for reading the paper, Phil Tunison and staff for drafting the figure, and Betty Williams for typing the manuscript.

The reviewers' comments were also very helpful in suggesting improvements in the presentation.

#### REFERENCES

1. S. CHANDRASEKHAR, "Hydrodynamic and Hydromagnetic Stability," Chapter III, Oxford Univ. Press, London, 1961.
2. F. B. LIPPS, *J. Fluid Mech.* **75** (1976), 113.
3. F. B. LIPPS AND R. C. J. SOMERVILLE, *Phys. Fluids* **14** (1971), 759.
4. R. D. RICHTMYER AND K. W. MORTON, "Difference Methods for Initial-Value Problems," pp. 176-178, 2nd ed., Interscience, New York, 1967.
5. P. J. ROACHE, "Computational Fluid Dynamics," pp. 61-62, Hermosa Publishers, Albuquerque, New Mexico, 1972.
6. H. T. ROSSBY, *J. Fluid Mech.* **36** (1969), 309.
7. R. C. J. SOMERVILLE, *Geophys. Fluid Dynamics* **2** (1971), 247.
8. R. C. J. SOMERVILLE AND F. B. LIPPS, *J. Atmospheric Sci.* **30** (1973), 590.
9. G. P. WILLIAMS, *J. Fluid Mech.* **37** (1969), 727.